Pure appl. geophys. 157 (2000) 1081–1096
0033–4553/00/081081–16 $ 1.50 + 0.20/0

Pure and Applied Geophysics

Analytical Solution for Testing Debris Avalanche Numerical Models

ANNE MANGENEY,[1,2] PHILIPPE HEINRICH[1] and ROGER ROCHE[1]

Abstract—We present here the analytical solution of a one-dimensional dam-break problem over inclined planes. This solution is used to test a numerical model developed for debris avalanches. We consider a dam with infinite length in one direction where material is released from rest at the initial instant. We solve analytically and numerically the depth-averaged long-wave equations derived in a topography-linked coordinate system. The numerical and analytical solutions provide for a Coulomb-type friction law at the base of the flow. The analytical solution is obtained by using the method of characteristics and describes the flow over a constant slope, provided that the angle is higher than the friction angle. The numerical model utilizes a finite-difference method based on a Godunov-type scheme. Comparison between analytical and numerical results illustrates the remarkable stability and precision of the numerical method as well as its ability to deal with strong discontinuities.

Key words: Analytical solution, shallow-water model, dam-break, debris avalanche.

1. Introduction

Gravitational flows such as water floods, landslides, debris avalanches and dense snow avalanches regularly cause substantial human and material damage. These flows are commonly generated by a sudden release from the rest of a fluid mass similar to a dam-break. We provide here a simple analytical solution for the dam-break problem which can be adopted to test numerical models dealing with such flows. A numerical method developed to model debris avalanches is also proposed and tested using this analytical solution.

Since the characteristic length of the flowing material is generally considerably larger than the fluid thickness, the long wave approximation has been widely applied in numerical models describing the dynamics of flow phenomena (e.g., HUNT, 1984, 1994; IVERSON, 1997; SAVAGE and HUTTER, 1989; HUTTER *et al.*, 1995). The models differ primarily in their representation of basal resistance forces and the constitutive relations describing the mechanical behavior of the considered

[1] Laboratoire de Détection et de Géophysique, CEA, Bruyères-le-Châtel, France. E-mail: anne.mangeney@ccr.jussieu.fr

[2] Now at Laboratoire d'Environnement et de Développement, Université Paris 7, Paris, France.

material. For landslides and debris and dense snow avalanches, uncertainties persist about the most appropriate flow law (viscous, Coulomb-type, Bagnold behavior) and basal friction law, both depending on the concentration of fluid, solid and gas within the flowing material (HUNT, 1984; LAIGLE and COUSSOT, 1997; ARATTANO and SAVAGE, 1994; MACEDONIO and PARESCHI, 1992; CHENG-LUN *et al.*, 1996; WHIPPLE, 1997). Therefore, depth-averaged models (i.e., hydraulic type models) provide a good way of assessing gravitational flow dynamics as they do not need a precise knowledge of the mechanical behavior within the flow. Also, depth-averaged models do not require large numerical resources and can be easily applied to real 3-D topography. We present here an analytical and numerical solution for depth-averaged long-wave equations derived in a linked-topography coordinate system with the possibility of taking into account a friction law at the base of the flow.

An analytical solution for the classic one-dimensional water flood created by dam failure over a horizontal plane without friction has been provided by STOCKER (1957). Approximate solutions have also been obtained for the dam-break problem in a prismatic, infinitely-long sloping channel (HUNT, 1982) and for dam-break flow in which the reservoir, dam breach, and downstream channel have different widths (HUNT, 1984), both without friction at the base of the flow. However, to the authors' knowledge, no analytical solution of the dam-break problem over an infinitely-long sloping channel has been provided to date. The analytical solution presented here is obtained by using the method of characteristics. The solution utilizes a Coulomb-type friction law at the base of the flow, provided that the angle of friction is smaller than the slope angle. The development of this analytical solution, although not straightforward, does not require complicated mathematics. This analytical solution does not include any flow law. Its major asset is to provide a test for numerical models of water flood when no friction is taken into account and of landslide, debris or dense snow avalanche problems when a Coulomb-type friction law is introduced.

The instantaneous release of fluid from rest, typical of these natural gravitational flows, leads to a significant initial discontinuity. Most numerical models developed for such flows fail to deal with this discontinuity and more generally with strong variations of the fluid height. Hence, several features of debris avalanches such as the formation of a surge and its breakup into multiple surges are generally not modelled accurately (IVERSON, 1997). We present here a numerical model based on a shock-capturing method, similar to those currently used to simulate compressible inviscid flows with shock waves. This model solves the St. Venant equations derived in a similar way by NAAIM *et al.* (1997) and LAIGLE and COUSSOT (1997).

In this paper we focus on the comparison between analytical and numerical results to assess the efficiency of the numerical model and in particular its ability to deal with large variations of the fluid height. In section 2 we present the system of equations, in section 3 we develop the analytical solution, in section 4 we describe the numerical model, and finally in section 5 we compare the results with the analytical solution.

2. Equations

The one-dimensional flow of an incompressible fluid is described by mass and momentum conservation equations. Gravitational flows are generally large and shallow so that the long-wave approximation along the slope is valid. We consider here the simple case of a uniform slope with an angle θ representing the topography (Fig. 1). A fluid is released from rest at the initial instant $t_0(u(x, t_0) = 0)$. The initial conditions are those of a dam of constant depth $h_0 = h(x, t_0)$ and an infinite length in the positive x-direction (Fig. 1).

The equations are obtained by depth-averaging Euler's equations for an incompressible fluid and by using the free surface boundary condition. The coordinate system is linked to the topography, (in our case x-axis is parallel to the uniform slope). Following NAAIM *et al.* (1997), Coulomb-type friction law has been introduced in our model to describe debris or dense snow avalanches. A simple representation of water flood is obtained when no friction is considered although more realistic models would include a resistance term at the base of the flow (HUNT, 1982). Mass and momentum equations can be written as

$$\frac{\partial u}{\partial t} + u\frac{\partial u}{\partial x} = -g\cos\theta\frac{\partial h}{\partial x} - g\sin\theta + F \tag{1}$$

$$\frac{\partial h}{\partial t} + \frac{\partial}{\partial x}(uh) = 0, \tag{2}$$

where u is the depth-averaged horizontal velocity, h the fluid height, g is the acceleration due to gravity ($g = 9.81\ \mathrm{ms}^{-2}$), and F the well-known Coulomb-type friction law

$$F = -g\cos\theta\ \mathrm{tg}\,\delta\ \mathrm{sgn}(u) \tag{3}$$

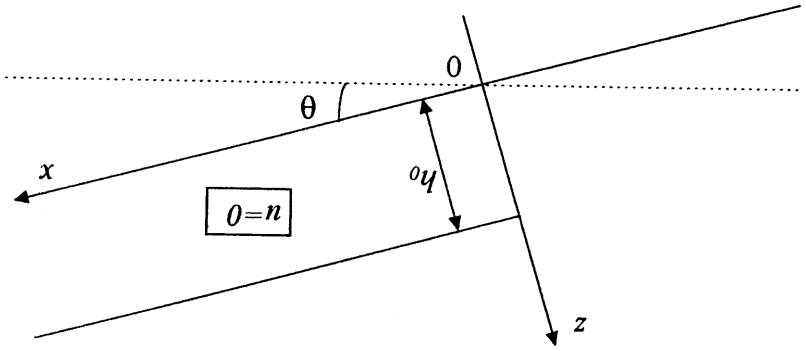

Figure 1
Dam-break geometry at the initial instant $t_0 = 0$ s.

where sgn is a function defining the sign of u, and δ is the dynamic friction angle ($20° < \delta < 40°$ for debris avalanche). If $\text{tg}\,\delta < \text{tg}\,\theta$, the fluid never stops on the inclined plane and F is always of the same sign, opposed to the sign of u. On the other hand, if $\text{tg}\,\delta > \text{tg}\,\theta$ the fluid may stop which results in discontinuous values of F. A criterion must then be imposed on the value of F depending on the force balance when the fluid stops. As a result, the case $\text{tg}\,\delta > \text{tg}\,\theta$ cannot be easily solved analytically. We focus here on the case $\text{tg}\,\delta < \text{tg}\,\theta$, so that $\text{sgn}(u) = -1$ and $F > 0$ at any time.

Equations (1)–(3) provide a simplified representation of debris and dense snow avalanche dynamics, in particular it does not include a constitutive relation for the fluid. However, this model gives a first approximation of the velocity and runout distance of debris avalanches (NAAIM *et al.*, 1997) and has the advantage of using only one parameter, the friction angle, that can be easily measured from laboratory experiments rather than numerically calibrated (IVERSON, 1997). It can be pointed out that the numerical model presented below can easily be extended to solve the equations developed by SAVAGE and HUTTER (1989) for Coulomb-frictional materials.

3. Analytical Solution

We solve analytically here equations (1) and (2) in the case of a friction angle δ lower than the slope angle θ, by employing the method of characteristics, following closely the approach of STOCKER (1957). The equations of mass and momentum can be written in terms of $\bar{p}$ and $\bar{\rho}$ defined as

$$\bar{\rho} = \rho h \tag{4}$$

$$\bar{p} = \frac{1}{2}\rho g \cos\theta h^2, \tag{5}$$

where ρ is the density of the incompressible fluid, so that Equations (1) and (2) become

$$\bar{\rho}\left(\frac{\partial u}{\partial t} + u\frac{\partial u}{\partial x}\right) = -\frac{\partial \bar{\rho}}{\partial x} + \bar{\rho} g \cos\theta \frac{\partial h_0}{\partial x} - \bar{\rho} g \sin\theta + \bar{\rho} F \tag{6}$$

$$\frac{\partial \bar{\rho}}{\partial t} + \frac{\partial}{\partial x}(u\bar{\rho}) = 0. \tag{7}$$

Note that in our case $\partial h_0/\partial x = 0$ (Fig. 1). When the three last terms of the right-hand member of (6) are equal to zero (i.e., when the flow depth height is constant, the topography is horizontal, $\theta = 0$, and no friction occurs at the base) the resulting system corresponds to the equations governing the evolution of an isentropic compressible fluid (in which the fluid height plays the role of density)

with an "adiabatic exponent" $\gamma = 2$. This formulation allows solution of the equations by analogy with compressible gas dynamics and to introduce a "sound wave velocity" defined as

$$c = \sqrt{\frac{d\bar{p}}{d\bar{\rho}}} = \sqrt{g \cos\theta h}. \tag{8}$$

The quantity c represents the local speed of propagation of "small disturbances" relative to the moving stream (STOCKER, 1957). By replacing h by c and by considering that $\partial h_0/\partial x = 0$, (6) and (7) now become,

$$\frac{\partial u}{\partial t} + u\frac{\partial u}{\partial x} + 2c\frac{\partial c}{\partial x} + g \sin\theta - F = 0 \tag{9}$$

$$2\frac{\partial c}{\partial t} + 2u\frac{\partial c}{\partial x} + c\frac{\partial u}{\partial x} = 0. \tag{10}$$

By adding (9) to (10) and subtracting (9) to (10), we obtain

$$\left[\frac{\partial}{\partial t} + (u + c)\frac{\partial}{\partial x}\right](u + 2c - mt) = 0 \tag{11}$$

$$\left[\frac{\partial}{\partial t} + (u - c)\frac{\partial}{\partial x}\right](u - 2c - mt) = 0, \tag{12}$$

respectively, with

$$m = -g \sin\theta + g \cos\theta \operatorname{tg}\delta, \tag{13}$$

which means that $k_+ = u + 2c - mt$ and $k_- = u - 2c - mt$ are constant along the characteristic curves C_+ and C_-, respectively, defined as

$$C_+: \quad \frac{dx}{dt} = u + c, \tag{14}$$

$$C_-: \quad \frac{dx}{dt} = u - c. \tag{15}$$

The systems (9, 10), (11, 12) and (14, 15) associated with the constant value of k_+ and k_- along the characteristics are equivalent. Note that the two families of curves C_+ and C_- are distinct only if c is not equal to zero, i.e., if the free surface never touches the bottom. In the case of dam-break over horizontal bottom, the family of characteristics C_+ consists entirely of straight lines passing through the origin, along each of which u and c are constant (COURANT and FRIEDRICHS, 1948).

Equations (14) and (15) can be solved analytically in the case of dam-break over an inclined plane and with a Coulomb type friction law (i.e., when m is a constant value). Dam-break corresponds to the initiation of a disturbance at the instant

$t_0 = 0$, propagating into a fluid flowing down with constant acceleration m. In the quiet region (i.e., where fluid remains unaffected by the disturbance) the fluid flows down at a velocity $u = mt$. As was done in STOCKER (1957), we define an "initial characteristic" which divides the quiet region from the disturbed region in the x, t-plane. In the case of horizontal dam-break, this characteristic corresponds to the curve $x = c_0 t$. In the quiet region $c = c_0$ and $u = mt$ and by integrating (14) the equation of C_+^0 reads

$$x = c_0 t + \frac{1}{2} m t^2. \tag{16}$$

We now consider a given characteristic C_+ in the x, t-plane and a point M on this characteristic. The flow being subcritical, the characteristic C_-^M issuing from M intersects the initial characteristic C_+^0 at the point N. By using the fact that k_- is constant on C_- and knowing the values of c and u on C_+^0 the following relation is obtained at the point M

$$u = 2c - 2c_0 + mt \tag{17}$$

so that (14a) reads

$$C_+ : \quad \frac{dx}{dt} = 3c - 2c_0 + mt. \tag{18}$$

On the other hand k_+ is constant on C_+ and by using (17) this implies that $2c - c_0$ is constant on C_+, so that c is constant on this characteristic. This property allows us to integrate (18) to obtain the values of u and c within the zone of disturbance

$$u = \frac{2}{3}\left(\frac{x}{t} - c_0 + mt\right), \tag{19}$$

$$c = \frac{1}{3}\left(\frac{x}{t} + 2c_0 - \frac{1}{2} mt\right). \tag{20}$$

From (20) the required analytical solution for the fluid height h is easily calculated

$$h = \frac{1}{9g \cos\theta}\left(\frac{x}{t} + 2c_0 - \frac{1}{2} mt\right)^2. \tag{21}$$

The formula (21) is valid outside the quiet region defined by $x > x_R = c_0 t + \frac{1}{2} m t^2$, where the fluid height is constant $h = h_0$ and upstream from the front of the fluid (i.e., $h = 0$) defined by $x_L = -2c_0 t + \frac{1}{2} m t^2$. Note that in our case, m being negative, x_L is negative for all values of t.

As a consequence, the equations of the characteristics can be easily obtained

$$C_+ : \quad \frac{dx}{dt} = \frac{x}{t} + \frac{1}{2} mt, \tag{22}$$

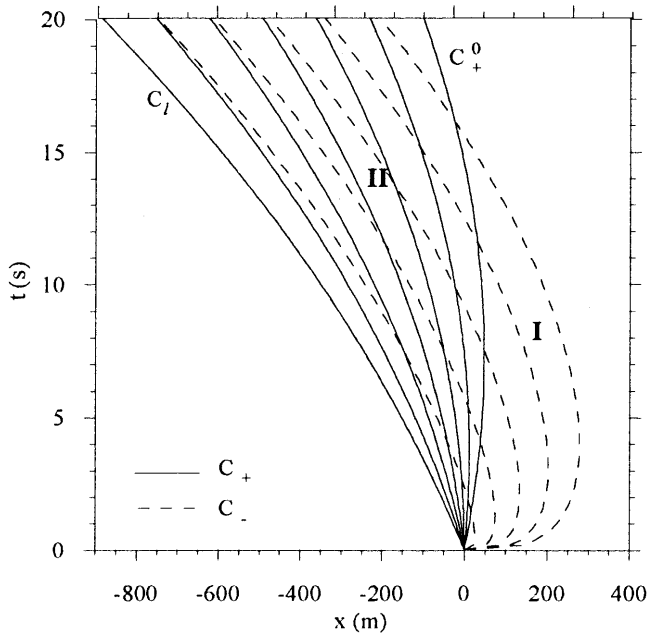

Figure 2
Characteristic curves C_+ and C_- in the x, t-plane for $\theta = 30°$ and $\delta = 20°$ ($m = -1.8$ ms^{-2}, $c_0 = 13$ ms^{-1}). Zone I, corresponding to $x > c_0 t + \frac{1}{2} m t^2$, is called the quiet region and zone II, corresponding to $-2c_0 t + \frac{1}{2} m t < x < c_0 t + \frac{1}{2} m t^2$, is the region of non-constant state.

$$C_-: \quad \frac{dx}{dt} = \frac{1}{3}\left(\frac{x}{t} - 4c_0 + \frac{5}{2} mt\right), \tag{23}$$

leading to

$$C_+: \quad x = K_+ t + \frac{1}{2} mt^2, \tag{24}$$

$$C_-: \quad x = K_- t^{1/3} - 2c_0 t + \frac{1}{2} mt^2, \tag{25}$$

where K_+ and K_- are constant on each curve of the family C_+ and C_-, respectively. The equation of the initial characteristic C_+^0 is obtained for $K_+ = c_0$. Note that for $K_+ = -2c_0$ and $K_- = 0$, the characteristic $C_- = C_+ = C_l$ defines the limit between the zone of disturbance II and the region where $h = 0$ (Fig. 2).

It is worth noticing that the solution (21) may be also obtained from the solution of the horizontal problem (i.e., $m = 0$) by a simple change of reference frame

$$X = x - \frac{1}{2} mt^2 \tag{26}$$

$$U = u - mt \tag{27}$$

where m is the acceleration of the reference frame, X and U are the horizontal coordinate and velocity in the new reference frame, respectively, Substitution of (x, u) by (X, U) in (11) and (12) leads to

$$\left[\frac{\partial}{\partial t} + (U + c)\frac{\partial}{\partial X}\right](U + 2c) = 0, \tag{28}$$

$$\left[\frac{\partial}{\partial t} + (U - c)\frac{\partial}{\partial X}\right](U - 2c) = 0. \tag{29}$$

These equations are those obtained for the horizontal dam-break problem for which the well-known solution is

$$h = \frac{1}{9g\cos\theta}\left(\frac{X}{t} + 2c_0\right)^2, \tag{30}$$

which is equivalent to equation (21).

To illustrate the behavior of the analytical solution, fluid heights are calculated from (21) in the case of the instantaneous release of an infinitely-long fluid mass of 20 m high on a dry inclined bottom ($\theta = 30°$) first without friciton ($\delta = 0°$), second with $\delta = 10°$ and finally with $\delta = 20°$, hereafter referred to as case 1, case 2 and case 3, respectively (Fig. 3). The solution is shown at two instants $t = 10$ s and $t = 15$ s. The value of the bed friction angle effects significantly the solution as it is pointed out by SAVAGE and HUTTER (1991). The fluid front travels a distance of nearly 40% less in case 3 compared with case 1. This suggests that the bed friction angle is a critical parameter when modelling debris or dense snow avalanches.

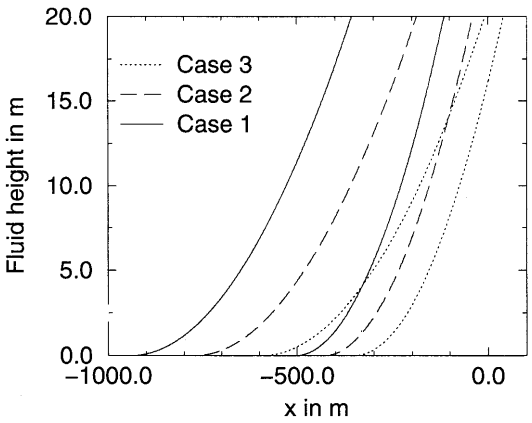

Figure 3
Fluid height obtained with the analytical solution versus distance from the initial edge of the dam for dam-break over a plane with slope angle $\theta = 30°$ without friction (case 1), with a friction angle $\delta = 10°$ (case 2), and with a friction angle $\delta = 20°$ (case 3). The solution is shown at two instants ($t = 10$ s and $t = 15$ s) in the three cases.

4. Description of the Numerical Model

We have used the analytical solution presented above to test a numerical model dealing with debris or dense snow avalanches when a Coulomb-type friction law is introduced and with water floods when no friction is taken into account. This model is not based on the method of characteristics. It solves equations (1) and (2) applying a finite-difference method based on a Godunov-type scheme.

Long-wave equations (1) and (2) are hyperbolic differential equations admitting discontinuous solutions which correspond to steep fronts or bores. These regions are characterized by strong gradients of velocities and flow heights which classic numerical schemes are not able to treat without producing numerical oscillations. In the case of negligible diffusion terms (such as viscosity) in the momentum equations, artificial viscosities are generally introduced (SAVAGE and HUTTER, 1989) or a filter is utilized to suppress numerical instabilities in the numerical solution. Hence IVERSON (1997) notes that most of the models fail when dealing with the downslope motion of surges at the front of debris flows or the breakup of a surge into multiple surges, for the distinction between numerical oscillations with physical instabilities is ambiguous.

In order to handle discontinuous solutions we have developed a shock-capturing method, similar to those currently used to simulate compressible inviscid flows with shock waves. The model is based on a high-order Godunov-type scheme. To our knowledge, this type of scheme has been applied to gravitational flows by only a few authors (e.g., NAAIM *et al.*, 1997; LAIGLE and COUSSOT, 1997; FRACCAROLLO and TORO, 1995). All these methods are Eulerian. The originality of our method is to use a Lagrangian approach before a projection on an Eulerian grid is carried out. Our method is especially well suited for the treatment of strong discontinuities. It is characterized by fact that the discontinuity is linked to a moving mesh point (COCCHI, *et al.*, 1996) and is accurately dealt with by using Rankine-Hugoniot formulas. Using the Lagrangian approach, equations (1) and (2) are expressed as follows

$$\frac{du}{dt} = -\frac{\partial p}{\partial x} - g \sin\theta + F \tag{31}$$

$$\frac{dM}{dt} = 0, \tag{32}$$

where M is the mass of the fluid, and p, hereafter called "pressure," is defined as

$$p = \frac{1}{2} g \cos\theta h^2. \tag{33}$$

The unknowns of the problem u and p are calculated at the cell centers.

The numerical scheme of our method consists of four steps. Firstly, a linear Rieman problem is solved to calculate velocities and pressures at the cell interfaces at time n from cell centered values. Secondly, the scheme is extended to second-order space using the concept of VAN LEER (1979) in which the quantities are not considered as constant inside each cell but vary as affine functions. Velocities and pressures at cell interfaces are thus corrected and calculated explicitly at an intermediate time $n+\frac{1}{2}$, which results in a second-order scheme in time. In order to suppress numerical oscillations generated at discontinuities by the second-order scheme, slope limiters are used for the velocity and pressure. The limiter concept allows one to derive a first-order stable solution for the discontinuities and a second-order solution elsewhere. The so-called "Superbee" limiter is used; it is a nonlinear function of the ratio of adjacent gradients and is known to propagate accurately discontinuous profiles over several characteristic lengths (ROE, 1985). The third step consists of solving equations (31) and (32). First, the displacements of mesh points are calculated using the latter interface velocities at time $n+\frac{1}{2}$. New fluid heights in the Lagrangian cells are then inferred from mass conservation (32). Second, new cell centered velocities at the time $n+1$ are calculated by solving the momentum equations (31). Finally, a projection of the quantities h and u is carried out on a fixed Eulerian grid, assuming that h and u vary as affine functions across each cell. The stability of the scheme is obtained with a time step satisfying the CFL condition (Courant-Friedrichs-Lewy).

If the second step is not carried out, one obtains a first-order Godunov's scheme. Due to the first-order accuracy in time and space, Godunov's model suffers from a relatively sizable numerical diffusion.

5. Comparison of Numerical and Analytical Solution

The existence of the analytical solution allows us to address the following issues: (i) what is the minimum grid step necessary to obtain an approximation of the solution at a given level of accuracy, (ii) does the second-order Van Leer's method provide more precise results than the first-order Godunov's method, (iii) what is the ability of the method to deal with discontinuities , (iv) does the numerical precision correspond to first-order for the discontinuities and to second-order elsewhere?

We shall consider here only the case of a horizontal bottom without basal friction corresponding to a simple representation of water flood over horizontal slope. Similar results are obtained for the flow over inclined planes with basal friction. The test case consists of the instantaneous release of a fluid mass of 20 m high on a dry flat bottom, infinitely-long in the positive x-direction. The numerical domain ranges from -1000 m to 1000 m. Note that the aspect ratio of the geometry considered here is $\epsilon = 2 \cdot 10^{-2}$, so that the long-wave approximation is valid. All numerical experiments are carried out with a time step $\Delta t = 0.01$ s.

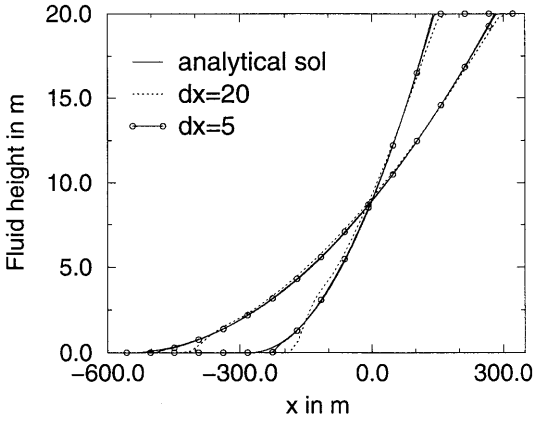

Figure 4
Fluid height versus distance from the initial edge of the dam obtained for $\delta = 0°$ and $\theta = 0°$, at $t = 10$ s and $t = 15$ s with the analytical solution (solid lines) and with Van Leer's method, for $\Delta x = 20$ m (dotted lines) and for $\Delta x = 5$ m (circle).

To test the numerical precision, we express the results in terms of the mean relative error Δh and the relative error at point x, δh, defined as

$$\Delta h = \frac{\sum (h - h_a)^2}{\sum h_a^2}, \tag{34}$$

$$\delta h = \frac{(h(x) - h_a(x))^2}{h_a(x)^2}, \tag{35}$$

where h_a is the analytical solution for h and Σ represents the sum over all the points at which $0 < h < h_0$. This numerical study will be carried out referring only to the error on h; similar results are obtained when the error on u is considered.

We first compare the numerical solution obtained with Van Leer's method with the analytical solution for various grid steps (Fig. 4). On this figure it can be observed that the numerical model presents a good representation of the dam-break problem. The numerical solution obtained with grid steps lower than 4 meters (i.e., 400 points for the computational domain) provides a good approximation of the exact solution with a mean relative error Δh lower than $5 \cdot 10^{-3}$. The main difference between analytical and numerical results is located at the front position $x = x_L$ and at the corner of the dam, $x = x_R$. Note that, referring to the analytical solution (21), at $x = x_R$, the first derivative of the fluid height is discontinuous whereas at $x = x_L$, only the second derivative is discontinuous.

Figure 5 illustrates the comparison between the Godunov's and Van Leer's methods, using a grid step Δx of 5, 2.5 and 1.25 meters. Figure 5a clearly shows the

higher efficiency of the Van Leer's method compared with the Godunov's method to solve the equations near the sharp variation of the fluid height at $x = x_R$. It can be observed whatever the cell size, that the corners at the right discontinuity of the dam are rounded by Godunov's method. The rounding may be accounted for by numerical diffusion inherent to the first-order scheme. At the front, $x = x_L$, differences between Van Leer's and Godunov's methods are less significant (Fig. 5b). A steep front appears in the numerical solution compared to the analytical solution in the close vicinity of $x = x_L$ for both methods. It is worth pointing out that the numerical solution both at the front and at the top is located upstream from the analytical solution. This is probably due to the smoothing of the initial

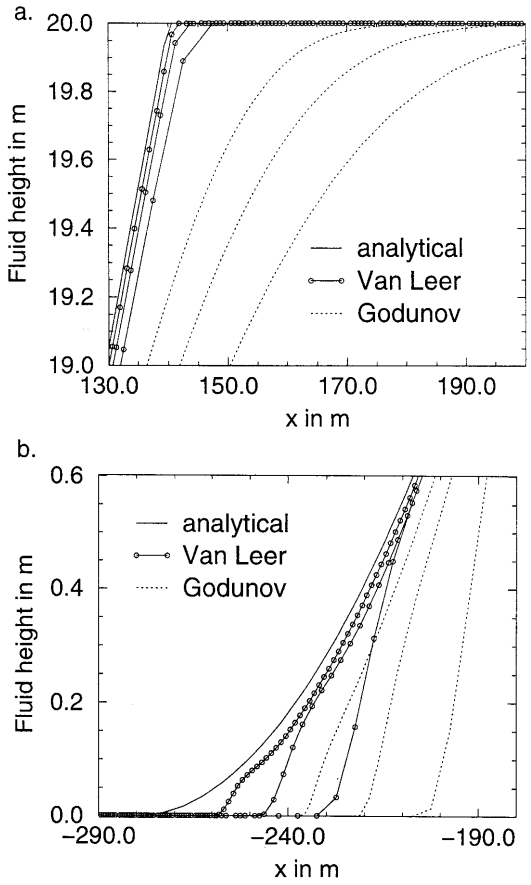

Figure 5

Fluid height versus distance from the initial edge of the dam obtained for $\delta = 0°$ and $\theta = 0°$, at $t = 10$ s, with analytical solution (solid lines), with Godunov's method (dashed-lines), and with Van Leer's method (circle), for $\Delta x = 5$, $\Delta x = 2.5$ m, $\Delta x = 1.25$ m, (a) near the top of the dam ($x = x_R$) and (b) near the front of the water ($x = x_L$). As Δx decreases, numerical solution is closer to the analytical solution, both with Van Leer's and Godunov's methods.

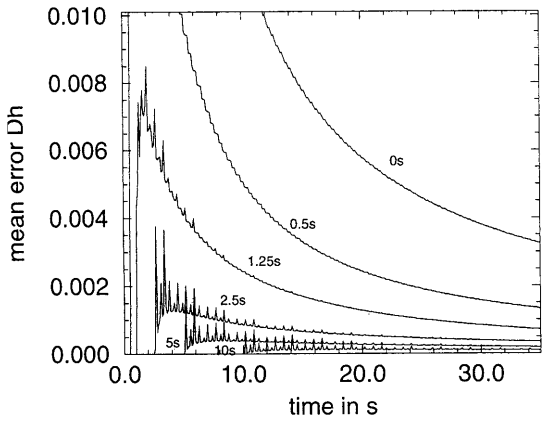

Figure 6
Mean relative error Δh is obtained for $\delta = 0°$ and $\theta = 0°$ versus time for initial condition taken as the analytical solution at $t_0 = 0$, $t_0 = 1.25$ s, $t_0 = 2.5$ s, $t_0 = 5$ s, and $t_0 = 10$ s.

discontinuity by the discretization, which leads to a slowing down of the fluid at the first instants.

The error due to the treatment of the initial discontinuity is assessed by performing a series of numerical experiments with the analytical solution $h_a(t_0)$ as initial condition, for different values of t_0. For $t_0 = 0$, the initial fluid height is discontinuous, whereas initial height gradients are smaller for increasing t_0. These tests are carried out with a grid step $\Delta x = 5$ m. Figure 6 depicts the relative mean error Δh as a function of time. For initial instant $t_0 = 0$, just after the fluid release,

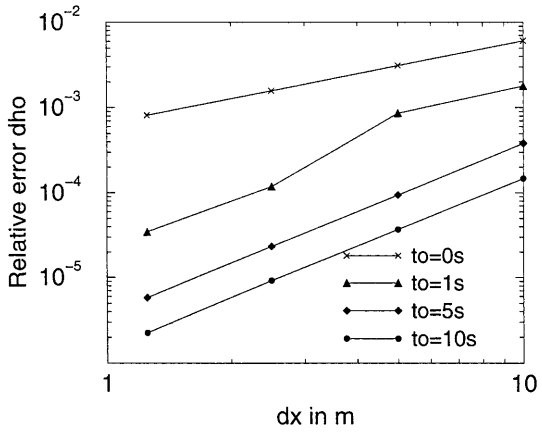

Figure 7
Relative error δh_0 obtained for $\delta = 0°$ and $\theta = 0°$ at $x = 0$ and at $t = 35$ s versus grid step Δx in log-log scale for various initial times t_0. Calculations have been carried out for $\Delta x = 10$ m (200 points), $\Delta x = 5$ m (400 points), $\Delta x = 2.5$ m (800 points), $\Delta x = 1.25$ m (1600 points).

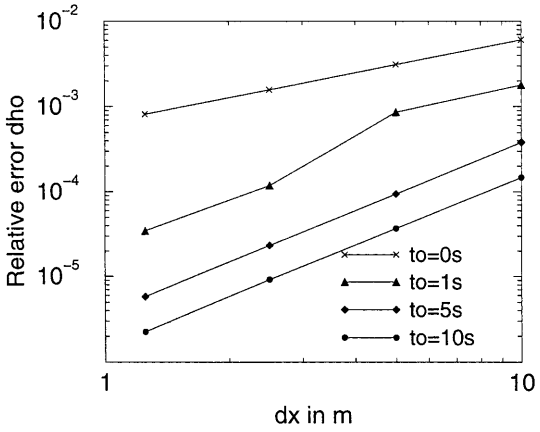

Figure 7
Relative error δh_0 obtained for $\delta = 0°$ and $\theta = 0°$ at $x = 0$ and at $t = 35$ s versus grid step Δx in log-log scale for various initial times t_0. Calculations have been carried out for $\Delta x = 10$ m (200 points), $\Delta x = 5$ m (400 points), $\Delta x = 2.5$ m (800 points), $\Delta x = 1.25$ m (1600 points).

the deviation from the analytical solution is very high with a maximum error $\Delta h = 0.2$ at $t = 0.1$ s $= 10\ \Delta t$, decreasing to $\Delta h = 0.1$ at $t = 0.2$ s. As time goes on, the error is lowered and tends towards a constant value. For increasing values of the initial instant t_0, the relative error decreases rapidly with time and, after 30 seconds, this error is smaller than 10^{-3} for $t_0 = 10$ s. These results demonstrate that the initial sharp variation of the fluid height pollutes the global solution. It appears that after 30 seconds the error is approximate inversely proportional to t_0. It can be explained by the fact that the fluid height variation is located in the interval $[x_R(t_0), x_L(t_0)]$, of which length is $x_L - x_R = 3c_0t_0 = n_0\Delta x$, where n_0 is the number of points located between $x_R(t_0)$ and $x_L(t_0)$. The error Δh seems to be roughly proportional to the number of points which describe the initial variation of h.

We now look at the order of the numerical scheme by calculating the error $\delta h_0 = \delta h(0)$ for grid steps ranging from $\Delta x = 10$ m to $\Delta x = 1.25$ m and for values of t_0 ranging from 0 s to 10 s. When starting from the initial discontinuity in h (i.e., $t_0 = 0$), the numerical precision corresponds to first order (Fig. 7). When increasing t_0 and for a small enough Δx, second order is obtained. For $t_0 = 1$ s, the numerical scheme precision corresponds to second order for $\Delta x < 2.5$ m and to first order for $\Delta x > 5$ m. For t_0 higher than 5 s, the numerical scheme is of second order for all grid steps considered here. For $\Delta x = 2.5$ m (i.e., 800 points), numerical tests reveal that the second order is obtained for t_0 approximate equal to 0.5 s. This result can be interpreted in terms of the required number points to accurately describe the initial condition. It seems that it is necessary to describe the initial variation of h between $x_R(t_0)$ and $x_L(t_0)$ with a minimum of approximately 10 points to provide the second-order numerical scheme.

Finally, the propagation of the error originating from the sharp edge at $x = x_R$ is illustrated in Figure 8 which shows the relative error δh at $x = 0$ m, $x = 50$ m and $x = -50$ m for $t_0 = 5$ s. This error reaches $x = 0$ m at $t = 9.4$ s, $x = 50$ m at $t = 12$ s, and $x = -50$ m, at $t = 6.4$ s. It propagates with a velocity equal to $(-u + c)$, confirming that c effectively represents the local speed of propagation of "small disturbance" relative to the moving stream.

6. Conclusion

We have presented here analytical and numerical solutions for 1-D flow of a fluid instantaneously released from rest. These solutions are obtained from depth-averaged long-wave equations derived in a linked-topography coordinate system. The analytical solution has been used to test the performance and precision of the numerical model.

The comparison between analytical and numerical results demonstrates the higher efficiency of Van Leer's method compared to Godunov's method. It has allowed us to assess the pollution of the "global" solution by the initial discontinuity, and leads to a precision of the numerical method corresponding to first order. We have shown, that when starting at later times, the accuracy becomes of second order. A minimum value of approximately 10 grid points describing the initial condition is required to obtain a second-order numerical scheme.

Van Leer's method used in our numerical model is remarkably stable and precise when dealing with significant discontinuities. The present model can be useful in practice for fluid flows in which nonlinear effects are important or in which strong changes (hydraulic jumps) are expected. This numerical model can be easily extended to solve more realistic equations such as those developed by SAVAGE and HUTTER (1989) for Coulomb-frictional materials. The analytical solution presented here may be useful to test numerical models which deal with gravitational flows such as water floods, landslides, debris or dense snow avalanches.

Acknowledgements

The present research has been supported by the DG XII of the Commission of the European Communities within the framework of the project GITEC (Genesis and Impact of Tsunamis on European Coasts). We thank the Institut de Physique du Globe de Paris for their facilities.

REFERENCES

ARATTANO, M., and SAVAGE, W. Z. (1994), *Modelling Debris Flows as Kinematic Waves*, Bull. Int. Assoc. Eng. Geol. *49*, 3–13.

CHENG-LUN, S., CHVAN-DENG, J., and YUAN-FAN, T. (1996), *A Numerical Simulation of Debris Flow and Its Application*, Natural Hazards *13*, 39–54.

COCCHI, J. P., SAUREL, R., and LORAUD, J. C. (1996), *Treatment of Interface Problems with Godunov-type Schemes*, Shock Waves *5*, 347–357.

COURANT, R., and FRIEDRICHS K. O., *Supersonic Flow and Shock Waves* (Interscience Publishers Inc., New York 1948).

FRACCAROLLO, L., and TORO, E. F. (1995), *Experimental and Numerical Assessment of the Shallow Water Model for Two-dimensional Dam-break Type Problems*, J. Hydraul. Res. *33*, 843–864.

HUNT, B. (1982), *Asymptotic Solution for Dam-break Problem*, J. Hydraul. Eng. *108*, HY1, 115–126.

HUNT, B. (1984), *Dam-break Solution*, J. Hydraul. Eng. *110* (6), 675–685.

HUNT, B. (1994), *Newtonian Fluid Mechanics Treatment of Debris Flows and Avalanches*, J. Hydraul. Eng. *120*, 1350–1363.

HUTTER, K., KOCH, T., PLUSS, C., and SAVAGE, S. B. (1995), *The Dynamics of Avalanches of Granular Materials from Initiation to Runout. Part II. Experiments*, Acta Mech. *109*, 127–165.

IVERSON, R. M. (1997), *The Physics of Debris Flows*, Rev. Geophys. *35* (3), 245–296.

LAIGLE, D., and COUSSOT, PH. (1997), *Numerical Modeling of Mudflows*, J. Hydraul. Eng. *123* (7), 617–623.

MACEDONIO, G., and PARESCHI, M. T. (1992), *Numerical Simulation of Some Lahars from Mount St. Helens*, J. Volcanol. Geotherm. Res. *54*, 65–80.

NAAIM, M., VIAL, S., and COUTURE, R. (1997), *Saint-Venant Approach for Rock Avalanches Modelling*, Saint Venant Symposium, August 28–29, Paris.

ROE, PH. L. (1985), *Some Contributions to the Modelling of Discontinuous Flows*, Lectures in Applied Mathematics *22*, 163–193.

SAVAGE, S. B., and HUTTER, K. (1989), *The Motion of a Finite Mass of Granular Material down a Rough Incline*, J. Fluid Mech. *199*, 177–215.

SAVAGE, S. B., and HUTTER, K. (1991), *The Dynamics of Avalanches of Granular Materials from Initiation to Runout. Part I: Analysis*, Acta Mech. *86*, 201–223.

STOCKER, J. J., *Water Waves*, *The Mathematical Theory with Applications* (Interscience Publishers, Inc., New York 1957).

VAN LEER, B. (1979), *Toward the Ultimate Conservation Difference Scheme V. A Second-order Sequel to Godunov's Method*, J. Comput. Phys. *32*, 101–136.

WHIPPLE, K. X. (1997), *Open-channel Flow of Bingham Fluids: Applications in Debris-flow Research*, J. Geol. *105*, 243–262.

(Received April 28, 1998, revised October 10, 1998, accepted October 30, 1998)